NATIONAL ADVISORY COMMITTEE FOR AERONAUTICS

TECHNICAL NOTE 3545

INVESTIGATION OF THE EFFECT OF SHORT FIXED DIFFUSERS ON STARTING BLOWDOWN JETS IN THE MACH NUMBER RANGE FROM 2.7 TO 4.5

By John A. Moore

Langley Aeronautical Laboratory
Langley Field, Va.

NACA

Washington

January 1956

NATIONAL ADVISORY COMMITTEE FOR AERONAUTICS

TECHNICAL NOTE 3545

INVESTIGATION OF THE EFFECT OF SHORT FIXED DIFFUSERS ON STARTING BLOWDOWN JETS IN THE MACH NUMBER RANGE FROM 2.7 TO 4.5

By John A. Moore

SUMMARY

An investigation was made at Mach numbers of 2.7, 3.0, 3.5, 4.0, and 4.5 to determine the effect of short fixed convergent-divergent wedge diffusers on the starting characteristics of blowdown jets exhausting to the atmosphere. Wedge diffusers that were extensions of the nozzle contours reduced the overall pressure ratios required for starting to less than one-half the values obtained without a diffuser. The minimum overall pressure ratio required for starting at each Mach number was about twice the value predicted by one-dimensional theory. Central-body diffusers were not so effective in reducing the overall pressure ratio for starting as were the wedge extensions of the nozzle, except at the higher values of diffuser minimum area. With the wedge extensions of the nozzle contours, the jets could be started for each test Mach number at values of diffuser minimum area that were considerably below the values predicted by one-dimensional theory. The jets could not be started for values of diffuser minimum area that were below those predicted by theory when central-body diffusers were used.

INTRODUCTION

In order to simplify the problem of model support for measurement of forces at angles of attack at high Reynolds numbers and supersonic speeds, two-dimensional nozzles exhausting the test-section flow directly (without diffusers) to the atmosphere can be used. This arrangement permits a relatively simple external model-support system which can take high aerodynamic loads at angles of attack.

In the Langley gas dynamics laboratory, it was found that such jets (or tunnels) could be started satisfactorily up to a Mach number of about 3.0. For higher Mach numbers, the stagnation pressures required for starting were excessive, on the order of five times the value predicted by one-dimensional theory for normal-shock starting, because of the separation of the boundary layer on the nozzle wall.

Various investigators have reported tests on pressure recovery during the starting of supersonic tunnels with long convergent-divergent diffusers. Eggink (ref. 1) describes the flow separation during starting in some of the tests first reported by Simons (ref. 2) and includes data on pressure recovery and minimum diffuser areas during starting of tunnels in the Mach number range from 1.6 to 2.5. Neumann and Lustwerk (ref. 3) reported data on pressure recoveries during starting for the Mach number range from 2.1 to 3.0. Diggins and Lange (ref. 4) investigated starting conditions as well as the effect of a variable-geometry diffuser on operating conditions in the Mach number range from 1.9 to 4.9. The same type of investigation was reported by Wegener and Lobb (ref. 5) in the Mach number range from 5.9 to 9.6. All these investigators reported pressure recoveries during starting of the tunnel that were close to those predicted by one-dimensional theory for nonviscous flow. One investigator, Fraser (ref. 6), reported tests on starting supersonic nozzles without diffusers. Fraser tested a three-dimensional nozzle at a Mach number of 3.35 and found that a pressure ratio across the nozzle of about seven times that predicted by one-dimensional theory was necessary to prevent detachment of the flow from the end of the nozzle.

Because of the lack of data on very short diffusers, the investigation reported herein was initiated to determine the effectiveness of several short convergent-divergent wedge diffusers in increasing the pressure recovery of supersonic nozzles during starting. The tests were made at Mach numbers of 2.7, 3.0, 3.5, 4.0, and 4.5 and Reynolds numbers, based on test-section height, of 7.83×10^6, 9.13×10^6, 10.67×10^6, 13.88×10^6, and 18.50×10^6, respectively.

SYMBOLS

A	cross-sectional area
M	Mach number
p	pressure
R	gas constant for air (1,715 sq ft/sec^2/$^\circ$F)
T	temperature, $^\circ$F abs
h	test-section height
l	length of convergent section of diffuser
m	length of divergent section of diffuser

q	free-stream dynamic pressure
u	local velocity of air
δ	diffuser-entrance wedge angle, see figure 2
β	diffuser-exit wedge angle, see figure 2
ρ	density
γ	ratio of specific heats, 1.400 for air

Subscripts:

o	stagnation conditions
o'	stagnation conditions at diffuser minimum-area section
1	conditions at test section (fig. 2); also conditions ahead of oblique shock
2	conditions behind oblique shock
a	atmospheric conditions
min	minimum

Superscripts:

$*$	conditions at nozzle minimum-area section
$*'$	conditions at diffuser minimum-area section

APPARATUS

The present investigation was conducted in the jet shown in figure 1, which is one of the facilities in the Langley gas dynamics laboratory. The jet is of the intermittent blowdown type and exhausts to the atmosphere. Dry air preheated to 100° F was supplied to the settling chamber at pressures up to 500 lb/sq in.

The supersonic nozzles used in the test were designed by the method of reference 7, and the design Mach numbers were 2.694, 3.012, 3.498, 4.012, and 4.515. Limited calibrations of the nozzles for $M = 3.012$ and $M = 4.012$ indicated test-section Mach numbers of 2.99 and 3.98, respectively. Static pressures measured along the side wall at the

other Mach numbers indicated close agreement between actual and design Mach numbers. The test section for each nozzle was 8 inches high and 9 inches wide, and the length of the supersonic portion of each nozzle was about 24 inches; the nozzle contours ended at the intersection of the contour with the Mach line representing the design Mach number.

Schematic diagrams of the test setups showing the geometry of the diffusers tested are shown in figure 2. All the diffusers tested were two-dimensional and were simple convergent-divergent wedges added either as extensions of the nozzle contours or as central-body diffusers. These short fixed convergent-divergent wedge diffusers will be referred to simply as short wedge diffusers. The central-body diffusers were tested only at $M = 4.0$. Three different values of the ratio of length of convergent diffuser to height of test section were tested: $l/h = 1$, $l/h = 2$, and $l/h = 3$. The total length of the diffuser section was $3h$, and, therefore, the values of the ratio of length of divergent diffuser to test-section height were: $m/h = 2$ for $l/h = 1$, $m/h = 1$ for $l/h = 2$, and $m/h = 0$ for $l/h = 3$. A longer divergent diffuser of length $9h$ was added at the end of the diffuser section in a series of tests at $M = 4.0$ only. In the tests without a diffuser, the side walls extended 6 inches beyond the end of the nozzle. The geometric relation between l/h, the diffuser-entrance angle δ, and the ratio of the diffuser minimum area to the test-section area $A^{*'}/A_1$ is given by the following expression:

$$\delta = \tan^{-1} \frac{1 - \frac{A^{*'}}{A_1}}{2\frac{l}{h}}$$

This relationship is plotted for convenience in figure 3. Since the wedge blocks were made reversible, the expression can also be used for the relation between m/h, the diffuser-exit angle β, and $A^{*'}/A_1$.

The schlieren system was a single-pass type with 18-inch-diameter mirrors and a General Electric B-H6 mercury lamp for a source. For the schlieren photographs, a flash with a duration of about 5 to 10 microseconds was used.

Static pressures were measured with mercury manometers which were accurate to within ± 0.05 inch. Stagnation pressures were measured on 16-inch dial gages of the precision Bourdon type which had ranges of 0 to 200 pounds per square inch for the lower pressures and 0 to 500 pounds per square inch for the higher pressures. Total pressures were measured on 16-inch dial gages of the precision Bourdon type which had a range of 0 to 100 pounds per square inch. These gages were accurate to within ± 0.5 percent of full-scale deflection.

TESTING METHODS

Static-pressure orifices were located along the side wall on the center line of the jet in the region of the test section and in the diffuser section. In order to aid in determining when supersonic flow was established in the test section and diffuser, total-pressure measurements were made in the test section and diffuser section about $1\frac{1}{2}$ inches from the side wall. In the test section, the total-pressure probes were located on the center line of the jet. In the diffuser section, the probes were located on the center line when the wedge extensions of the nozzle contour were installed, but were midway between the wedge diffuser and the nozzle extensions when the central-body diffusers were tested.

In making a particular test, the stagnation pressure was gradually increased until observation of the schlieren system image and measurements of the total pressure determined when supersonic flow was established in the test section. A visual record was made of the stagnation pressure at that moment. When schlieren photographs were taken, the stagnation pressure was held constant at the given value for about 20 seconds.

Schlieren photographs were taken of the flow in both the supersonic nozzle and the diffuser. In order to permit viewing of the supersonic nozzle and the diffuser, the nozzle blocks had to be moved with respect to the side walls since there was only one set of windows in the side wall. (See fig. 1.)

RESULTS AND DISCUSSION

Boundary-Layer Separation on Nozzle Contour

Schlieren photographs of the starting flow through an $M = 3.0$ nozzle without a diffuser (fig. 4) show that separation of the boundary layer from the nozzle contour occurs and that, as the stagnation pressure is increased, the point of separation moves downstream. In determining the pressure behind the separation shock, it is interesting to compare the results of two of the methods available for calculating this pressure. A compilation of data on the pressure coefficient associated with the separation of a turbulent boundary layer at various Mach numbers is presented in reference 8. In using these data, the pressure coefficients were converted to the ratio of the pressure behind the shock to the stagnation pressure. The equation of the line representing step data in figure 8 of reference 8 was

$$\frac{\Delta p}{q_1} = -0.086(M_1 - 5.9) \tag{1}$$

Converting $\Delta p/q_1$ to a pressure ratio and simplifying gives

$$\frac{p_2}{p_o} = \frac{p_1}{p_o}\left(1 + 0.357M_1^2 - 0.060M_1^3\right) \tag{2}$$

Equation (2) is plotted in figure 5 as the solid line.

The results of determining the pressure behind the separation shock by measuring the angle of the shock, with the local design Mach number and flow angle known, are shown in figure 5 and compare favorably with the data of reference 8.

The effectiveness of wedges added to the end of the nozzle contour in reducing the pressure downstream of the separation shock can be seen in figure 6. The separation of the boundary layer has moved downstream considerably as compared with the configuration without a diffuser (fig. 4) at equivalent values of stagnation pressure. The flow downstream of the separation is divided into a supersonic high-energy region and a low-energy region, with a mixing zone in between. The low-energy region shown in figure 4 is essentially at atmospheric pressure. Mixing with the supersonic region tends to lower this pressure, but backflow from the tunnel exhaust keeps the pressure high. The wedges added to the end of the tunnel reduce this backflow considerably and allow the pressure in the low-energy region to be lowered by the mixing action with the supersonic jet. If this pressure is lowered sufficiently, the shock system will move into the diffuser and the tunnel will start. (Compare figs. 4(b) and 6(b) at $p_o/p_a = 4.43$ and figs. 4(c) and 6(d) at $p_o/p_a = 6.47$.)

Results of Tests

The results of tests to determine the effect of varying the length and minimum area of the short wedge diffusers for various Mach numbers are given in figure 7 which shows, for each of the Mach numbers tested, the variation of the overall pressure ratio p_o/p_a required for starting with the ratio of diffuser minimum area to test-section area $A^{*'}/A_1$. As the value of $A^{*'}/A_1$ is decreased, the value of p_o/p_a required for starting is reduced until a certain minimum value is reached. Any further reduction in $A^{*'}/A_1$ then increases the value of p_o/p_a. The only exception occurs for the diffuser with $l/h = 3$, $m/h = 0$ which was

tested at $M = 4.0$ only. For this diffuser, as the value of $A^{*'}/A_1$ was decreased, the value of p_o/p_a required for starting decreased until $A^{*'}/A_1$ reached a value slightly smaller than the minimum predicted by one-dimensional theory. At this point a small decrease in $A^{*'}/A_1$ caused a large increase in p_o/p_a, followed by a gradual decrease in p_o/p_a as $A^{*'}/A_1$ was reduced further. The explanation for this shift in the curve could not be determined from the data obtained in this investigation.

Also shown in figure 7 are the data obtained for central-body diffusers at $M = 4.0$. The variation of starting pressure ratio for these diffusers shows the same general trend as for the wedge extensions of the nozzle contours. However, the tunnel would not start with the central-body diffusers for values of $A^{*'}/A_1$ below about 0.68. The explanation seems to be that the central-body diffusers split the flow into two channels and the asymmetric nature of the starting flow reduced the effectiveness of the interaction between the high-energy and low-energy regions of the jet. The central-body diffusers were generally not so effective in reducing the overall pressure ratio required for starting as were the wedge extensions of the nozzles. Only at the higher values of $A^{*'}/A_1$ were the central-body diffusers more effective than the wedges.

Figure 7 shows that a minimum value of $A^{*'}/A_1$ is obtained at each Mach number for which the tunnel could be started with different wedge diffusers. This minimum value of $A^{*'}/A_1$ is shown as a function of Mach number in figure 8. The one-dimensional theory (see fig. 8) is based on the assumptions of normal-shock losses at the entrance of the diffuser and sonic flow at the minimum diffuser area. Experimental values of $\left(A^{*'}/A_1\right)_{min}$ lower than theory predicts indicate that, from continuity considerations, losses upstream of the diffuser minimum-area section are much less than normal-shock losses and are probably taken through a series of oblique shocks. (See figs. 10 to 14.) The data of reference 5 which are shown in figure 8 for the range $M = 7.2$ to 9.6 are a reasonable extrapolation of the data obtained in this investigation. The data from reference 4, for the range $M = 1.86$ to 4.92, show considerably higher values of $\left(A^{*'}/A_1\right)_{min}$ for starting, and the data from reference 9 agree well with the results reported herein for $M = 3.0$. The tests reported in references 4 and 9 were made in two-dimensional tunnels using atmospheric stagnation conditions and a vacuum vessel at the exhaust. In reference 9, the throat location for values of $\left(A^{*'}/A_1\right)_{min}$

for starting was determined to be $l/h = 2.16$, the lowest value tested, and the throat location for optimum pressure recovery was $l/h = 4.83$. In reference 4, the values of $\left(A^{*'}/A_1\right)_{min}$ for starting were determined with the throat located at the position for optimum pressure recovery, which, for $M = 2.83$, was $l/h = 5.29$. It is felt that better agreement of the data in reference 4 with the results of both the present investigation and reference 9 would have occurred had values of $\left(A^{*'}/A_1\right)_{min}$ for starting been determined for various values of throat location. The Reynolds numbers of the tests of references 4 and 9 were approximately the same. In reference 4, the Reynolds numbers based on test-section height ranged from 2.5×10^6 at $M = 1.86$ to 0.6×10^6 at $M = 4.92$. In the present investigation, the Reynolds numbers based on test-section height ranged from 7.8×10^6 at $M = 2.7$ to 18.5×10^6 at $M = 4.5$.

The minimum values of p_o/p_a required for starting various Mach number nozzles are shown in figure 9. The values of p_o/p_a obtained with short wedge diffusers are approximately twice the values predicted by one-dimensional theory. Most of the losses occur downstream of the minimum diffuser area since the velocity energy of the stream is not efficiently recovered. This is verified also by the data in figure 8 since low values of $A^{*'}/A_1$ can be obtained only with low loss in energy upstream of the diffuser minimum area. Some tests made at $M = 4.0$ with an $m/h = 10$ subsonic diffuser downstream of the short convergent wedges gave values of p_o/p_a for starting near those for normal-shock recovery. A comparison of the data in figure 9 for the nozzle without a diffuser and for the nozzles with short wedges shows that the addition of short wedges reduces the value of p_o/p_a required for starting to less than one-half that for nozzles without diffusers.

Analysis of Flow During Starting Process

Figures 10 to 14 show the flow through the diffusers of various Mach number tunnels during starting, and figure 15 shows the flow through the nozzle of an $M = 4.0$ tunnel during starting. A study of these figures indicates a possible explanation for the low values of $A^{*'}/A_1$ and the high values of p_o/p_a obtained in this investigation. At low values of stagnation pressure, the pressure rise necessary to satisfy the condition of high pressure at the tunnel exit causes the boundary layer to separate far upstream along the nozzle contours. The separation takes place farther upstream on one contour than on the other. As the stagnation

pressure is increased, the separation moves downstream; when it reaches the vicinity of the diffuser, the flow suddenly changes to a symmetrical separation, which occurs on both nozzle contours at the same axial position. (See figs. 6 and 15.) The separation, with the resultant strong oblique shocks, moves to the entrance of the diffuser (see figs. 10 to 14) as the stagnation pressure is increased further.

The conditions of the flow at the diffuser minimum area can be studied with the aid of the continuity equation. The continuity equation for the nozzle minimum area and the diffuser minimum area is

$$\rho^{*}u^{*}A^{*} = \rho^{*'}u^{*'}A^{*'} \tag{3}$$

Substituting

$$u = M\sqrt{\gamma RT}$$

and

$$\rho = \frac{p}{RT}$$

for u and ρ in equation (3) gives

$$\frac{p^{*}}{p_{o}}\sqrt{\frac{T_{o}}{T^{*}}}\,M^{*}A^{*} = \frac{p^{*'}}{p_{o}}\sqrt{\frac{T_{o}}{T^{*'}}}\,M^{*'}A^{*'} \tag{4}$$

If sonic flow is assumed at the nozzle minimum area ($M^{*} = 1$), then equation (4) becomes

$$\frac{A^{*'}}{A_{1}}\frac{A_{1}}{A^{*}}\frac{p_{o}'}{p_{o}}\left(\frac{p^{*'}}{p_{o}'}\sqrt{\frac{T_{o}}{T^{*'}}}\,M^{*'}\right) = \text{Constant} \tag{5}$$

The variation of $\frac{p^{*'}}{p_{o}'}\sqrt{\frac{T_{o}}{T^{*'}}}\,M^{*'}$ with $M^{*'}$ is given in figure 16. The mass-flow parameter reaches a maximum at $M^{*'} = 1.0$ and falls off rapidly as $M^{*'}$ increases or decreases. When equation (5) is used in the present analysis, the values of the parameters involved in equation (5) must be considered average values at the cross section involved.

A study of the schlieren photographs of the flow through the diffuser at the condition just before the tunnel starts shows strong oblique

shocks at the entrance of the diffuser. The large deflections associated with the strong oblique shocks and the separated regions at the entrance of the diffuser give values of effective $A^{*'}/A_1$ that are much lower than the geometric $A^{*'}/A_1$. The total-pressure recovery must be high to satisfy equation (5). As the stagnation pressure is increased, but before the tunnel starts, the pressure rise across the shocks becomes less, the shocks become weaker (see schlieren photographs in figs. 11(a) and 14(b)), and a larger effective $A^{*'}/A_1$ results. When the stagnation pressure is increased to a high enough value, the pressure rise across the shock becomes low enough that the boundary layer will not separate and the flow becomes attached to the diffuser surface.

For a given stagnation pressure before the tunnel starts, a decrease of the geometric $A^{*'}/A_1$ reduces the area of the separated or low-energy region near the surface at the diffuser minimum area. This reduction of the low-energy region lowers the pressure gradient along the diffuser-entrance wedge and the flow will attach at a lower value of stagnation pressure. As the value of the geometric $A^{*'}/A_1$ is decreased further, a point will be reached where the low-energy region is negligible and the effective $A^{*'}/A_1$ approaches the geometric $A^{*'}/A_1$. In order for equation (5) to be satisfied, the average Mach number at the minimum diffuser area must be decreased, with stronger oblique shocks at the diffuser entrance. An increase in the stagnation pressure is then necessary to reduce the pressure rise across the shock to a value below that which will separate the boundary layer before the tunnel will start. This would explain the portions of the curves in figure 7 in which the pressure ratio p_o/p_a increases when $A^{*'}/A_1$ is decreased below a certain value, as is also evidenced by the schlieren photographs in figures 11(a) to 11(c).

The lower losses associated with oblique shocks permit values of $A^{*'}/A_1$ to be obtained that are considerably lower than one-dimensional theory predicts. With such low losses upstream of the minimum diffuser area, low values of overall pressure ratio should result. However, the determining factor is the pressure ratio necessary to overcome the adverse pressure gradient that causes separation of the boundary layer. If some means such as boundary-layer suction were used to reduce this adverse pressure gradient, it is probable that values of overall pressure ratios lower than theoretical values could be obtained.

CONCLUSIONS

An investigation made at Mach numbers of 2.7, 3.0, 3.5, 4.0, and 4.5 to determine the effects of short fixed convergent-divergent wedge diffusers on the starting characteristics of blowdown jets exhausting to the atmosphere indicated the following conclusions:

1. The addition of short wedges as extensions of nozzle contours to act as supersonic diffusers reduced the overall pressure ratios necessary to develop supersonic flow in jets from approximately five to a minimum of about two times the values predicted by one-dimensional theory over the range of Mach numbers tested.

2. At a Mach number of 4.0, the addition of a relatively long subsonic diffuser to the short wedge diffuser reduced the overall pressure ratio for starting to a value slightly higher than that given by one-dimensional theory.

3. Wedges used as central-body diffusers at a Mach number of 4.0 were generally not so effective in reducing the overall pressure ratio required for starting as were the wedge extensions of the nozzles. Only at the higher values of diffuser minimum area were the central-body diffusers more effective.

4. Wedge diffusers used as extensions of the nozzle contours permitted values of diffuser minimum area that were considerably below those predicted by one-dimensional theory. Central-body diffusers did not.

5. Wedges that were extensions of the nozzle contours were effective in reducing the extent of the separation of the turbulent boundary layer along the nozzle contours.

Langley Aeronautical Laboratory,
National Advisory Committee for Aeronautics,
Langley Field, Va., September 20, 1955.

REFERENCES

1. Eggink, [H.]: Strömungsaufbau und Druckrückgewinnung in Überschallkanälen. (Flow Structure and Pressure Recovery in Supersonic Tunnels.) FB Nr. 1756, Deutsche Luftfahrtforschung (Berlin-Adlershof), 1943. (Also available as Univ. of Michigan Translation (Bur. Aero. Contract No. NOa(s) 7964)).

2. Simons, F. P.: Untersuchungen an Diffusoren für Überschall-Windkanäle. Part I. FB Nr. 1738, Aerodynamisches Institut der Technischen Hochschule (Aachen), Jan. 16, 1943.

3. Neumann, E. P., and Lustwerk, F.: Supersonic Diffusers for Wind Tunnels. Jour. Appl. Mech., vol. 16, no. 2, June 1949, pp. 195-202.

4. Diggins, J. L., and Lange, A. H.: A Systematic Study of a Variable Area Diffuser for Supersonic Wind Tunnels. NAVORD Rep. 2421, U. S. Naval Ord. Lab. (White Oak, Md.), Dec. 1952.

5. Wegener, Peter P., and Lobb, R. Kenneth: NOL Hypersonic Tunnel No. 4 Results II: Diffuser Investigation. NAVORD Rep. 2376, U. S. Naval Ord. Lab. (White Oak, Md.), May 5, 1952.

6. Fraser, R. P.: Jet Research. Flow Through Nozzles at Supersonic Speeds - Interim Reports for July 1940 - June 1941. WA-1513-1a(3), Imperial College of Science (British), 1941.

7. Beckwith, Ivan E., and Moore, John A.: An Accurate and Rapid Method for the Design of Supersonic Nozzles. NACA TN 3322, 1955.

8. Lange, Roy H.: Present Status of Information Relative to the Prediction of Shock-Induced Boundary-Layer Separation. NACA TN 3065, 1954.

9. Patterson, A. M.: Factors Affecting the Performance of Supersonic Diffusers. UTIA Rep. No. 23, Univ. of Toronto, Inst. Aerophysics, Dec. 1952.

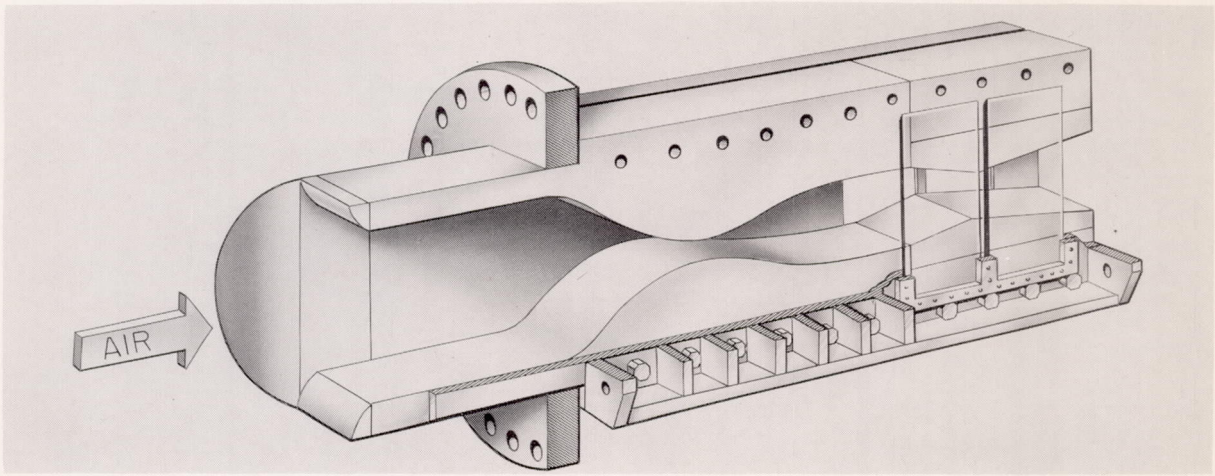

L-89323

(a) Schlieren windows opposite diffuser.

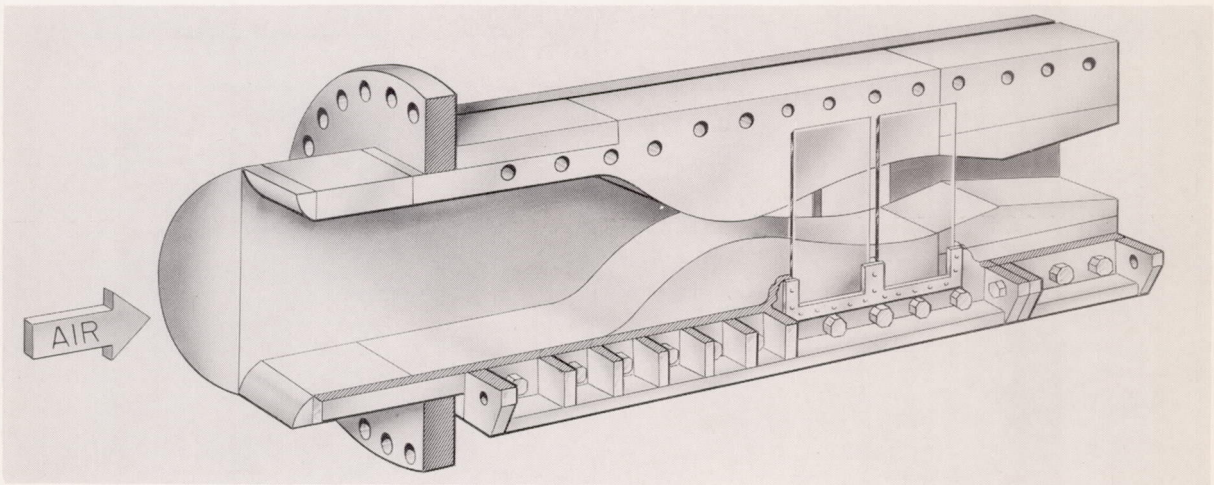

L-89324

(b) Schlieren windows opposite nozzle.

Figure 1.- Blowdown jet used in tests.

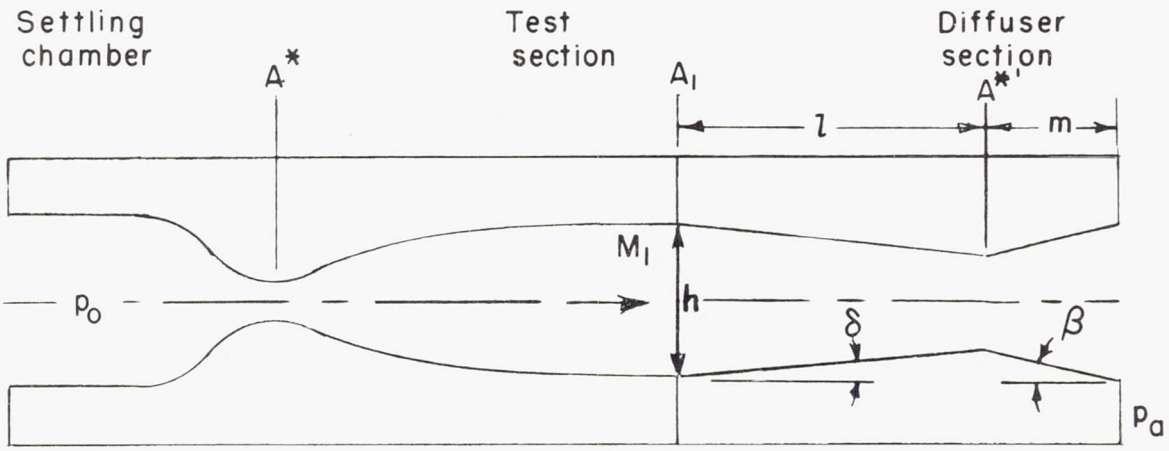

(a) Configuration with wedge diffusers as extensions of nozzle contours.

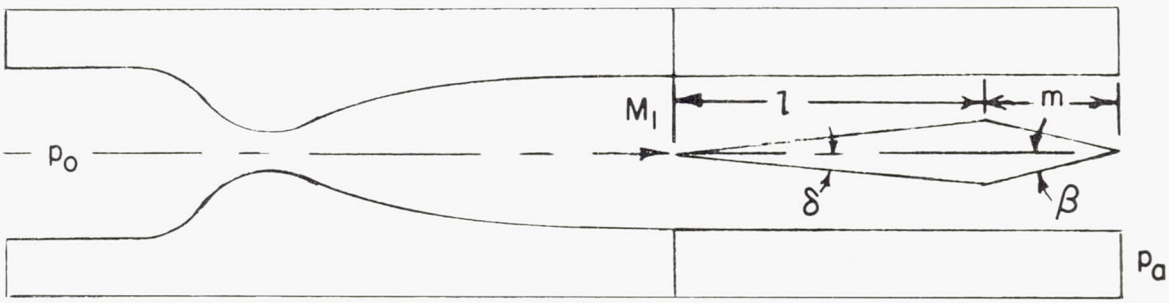

(b) Configuration with central-body diffusers.

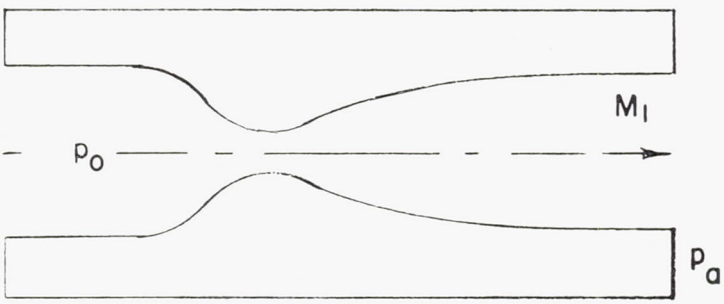

(c) Configuration without diffusers.

Figure 2.- Schematic diagrams of test setups.

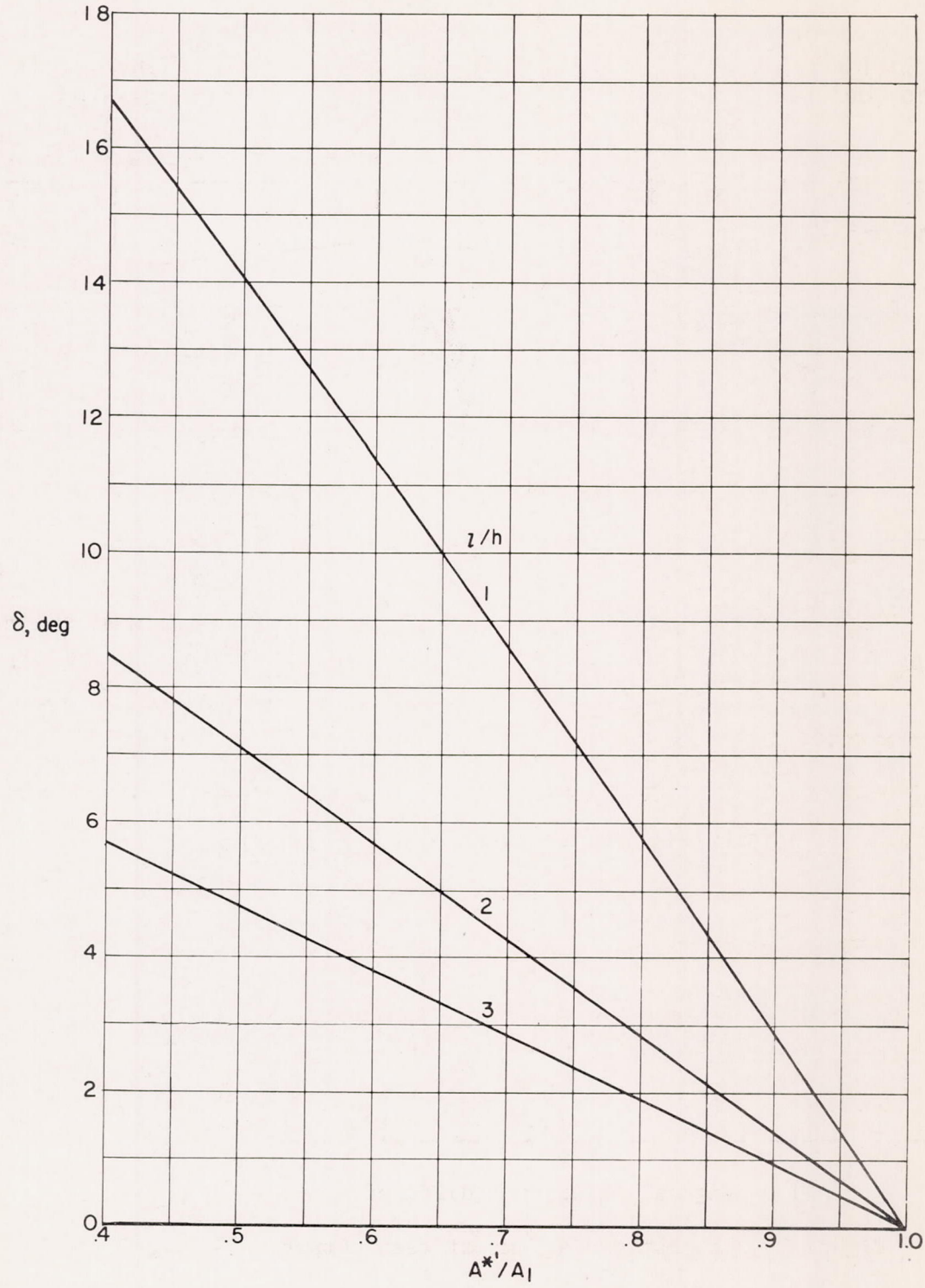

Figure 3.- Geometric relation between diffuser entrance angle and ratio of diffuser minimum area to test-section area for diffusers of given length.

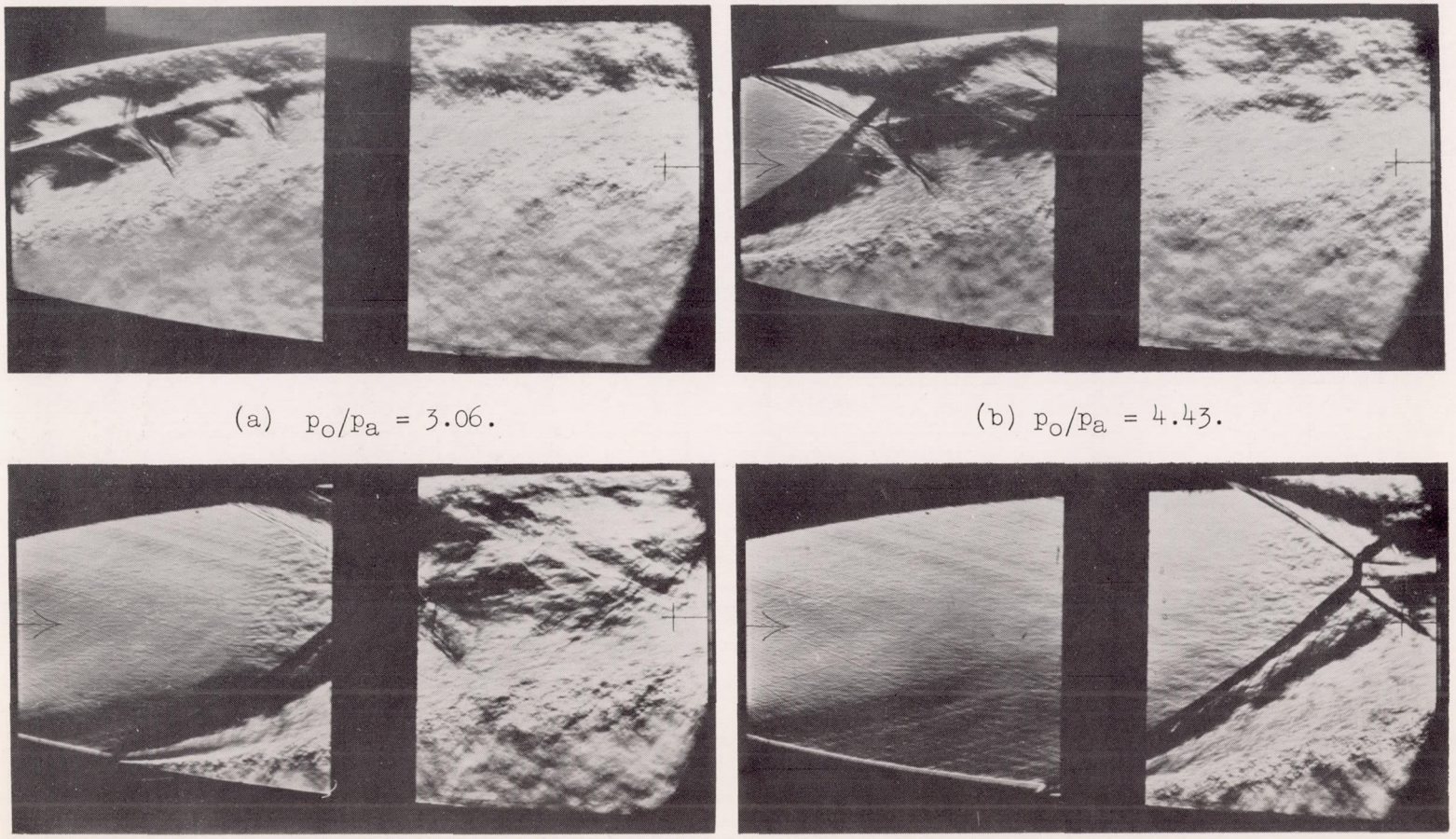

(a) $p_o/p_a = 3.06$.

(b) $p_o/p_a = 4.43$.

(c) $p_o/p_a = 6.47$.

(d) $p_o/p_a = 7.83$.

L-89325.1

Figure 4.- Starting flow in M = 3.0 nozzle without diffuser.

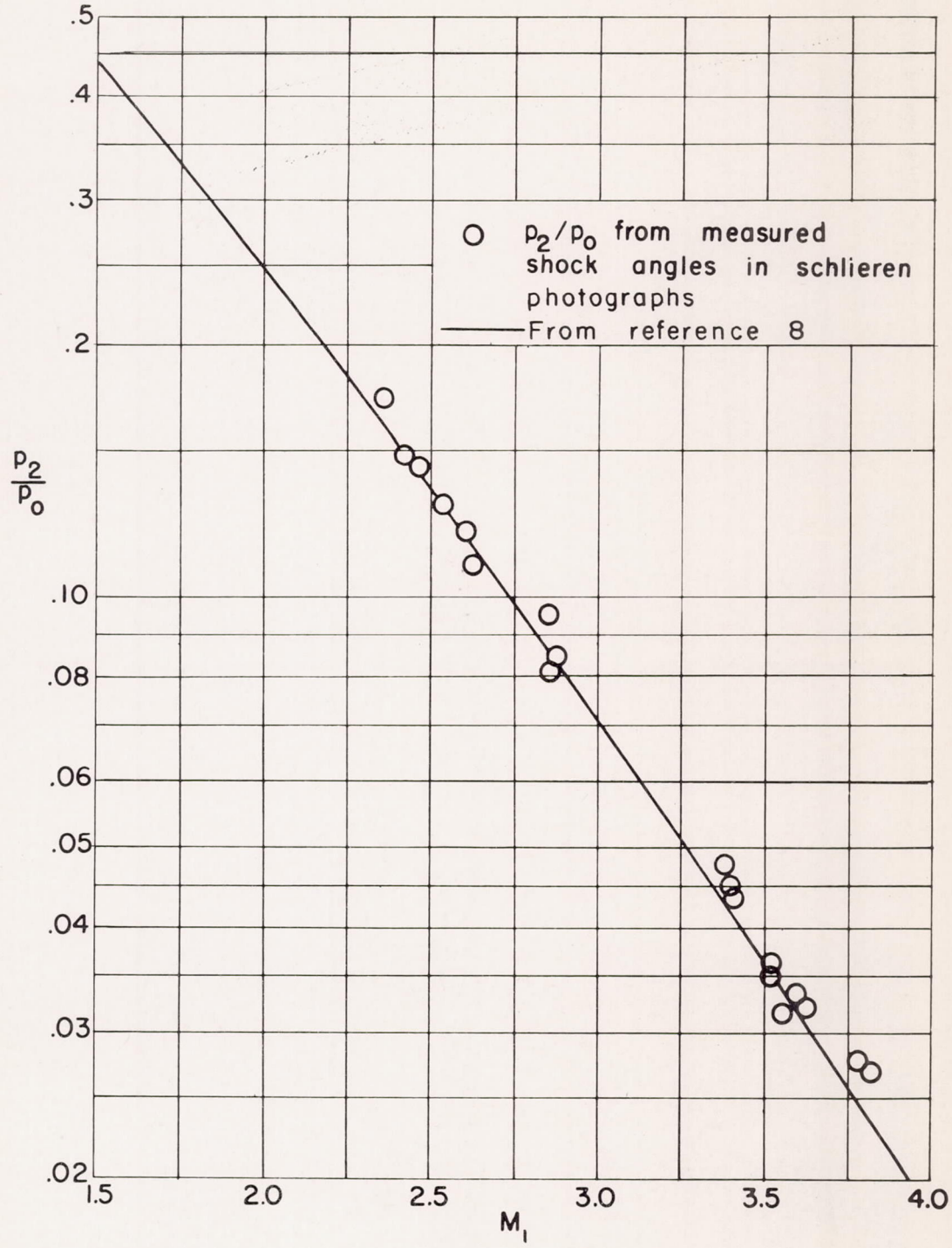

Figure 5.- Ratio of static pressure behind shock to stagnation pressure at Mach number ahead of shock for separated turbulent boundary.

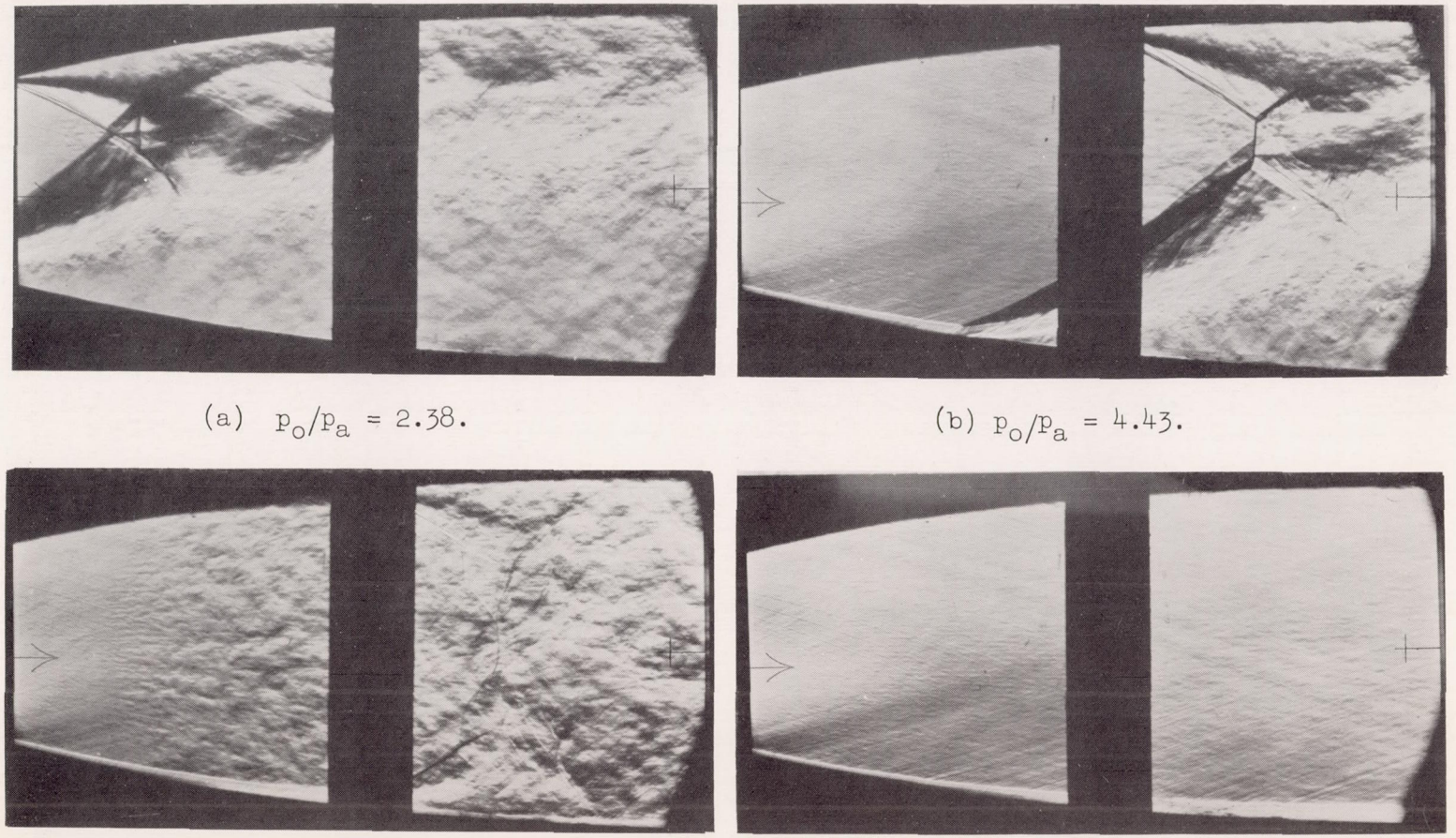

(a) $p_o/p_a = 2.38.$

(b) $p_o/p_a = 4.43.$

(c) $p_o/p_a = 4.77.$

(d) $p_o/p_a = 6.47.$

L-89326.1

Figure 6.- Starting flow in M = 3.0 nozzle with wedge diffuser. $l/h = 2$; $A^{*'}/A_1 = 0.652$.

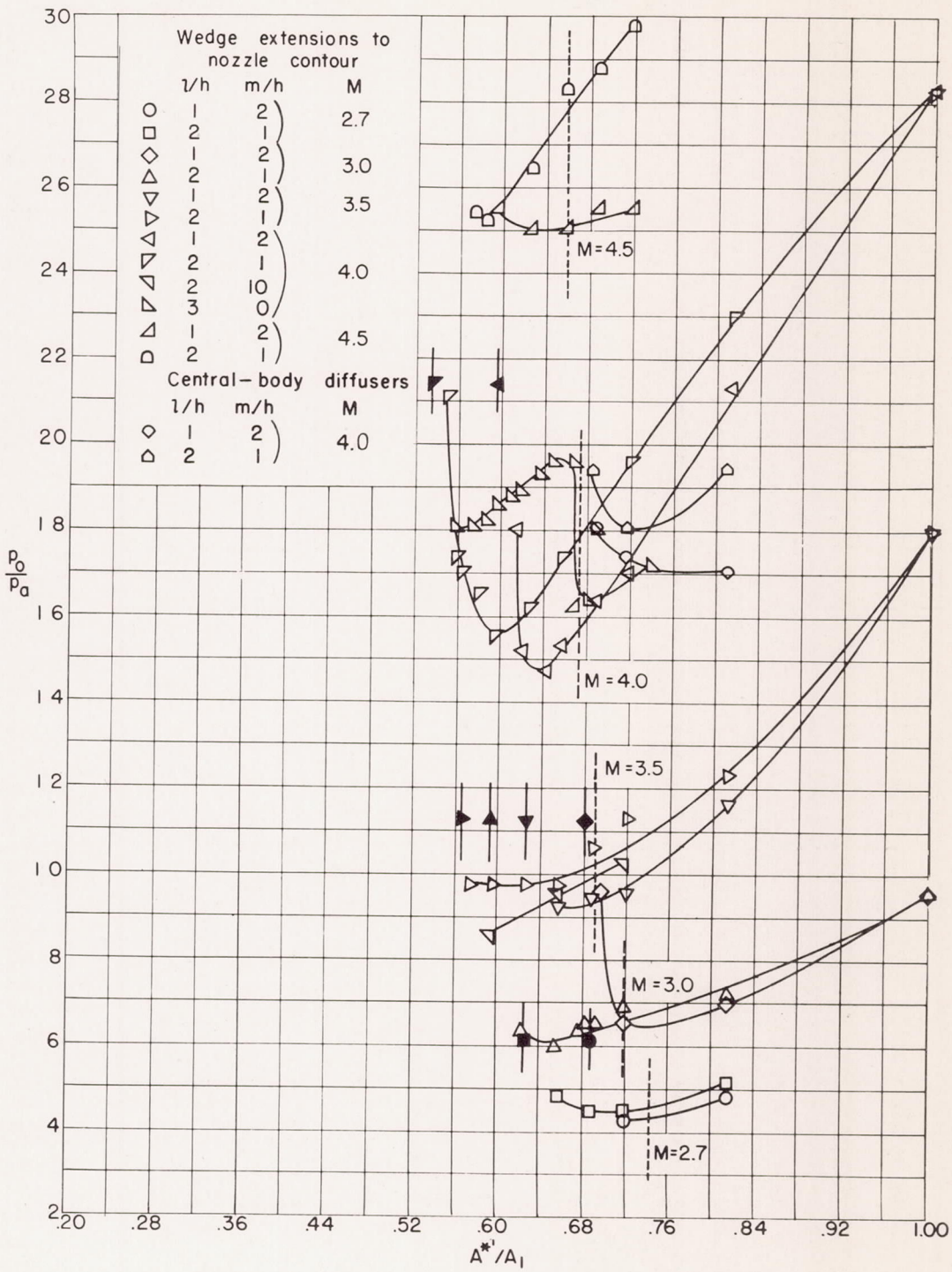

Figure 7.- Variation of overall pressure ratio required for starting with ratio of diffuser minimum area to test-section area. Solid symbols indicate conditions for which tunnel did not start. Dashed lines indicate $\left(A^*/A_1\right)_{min}$ from one-dimensional theory.

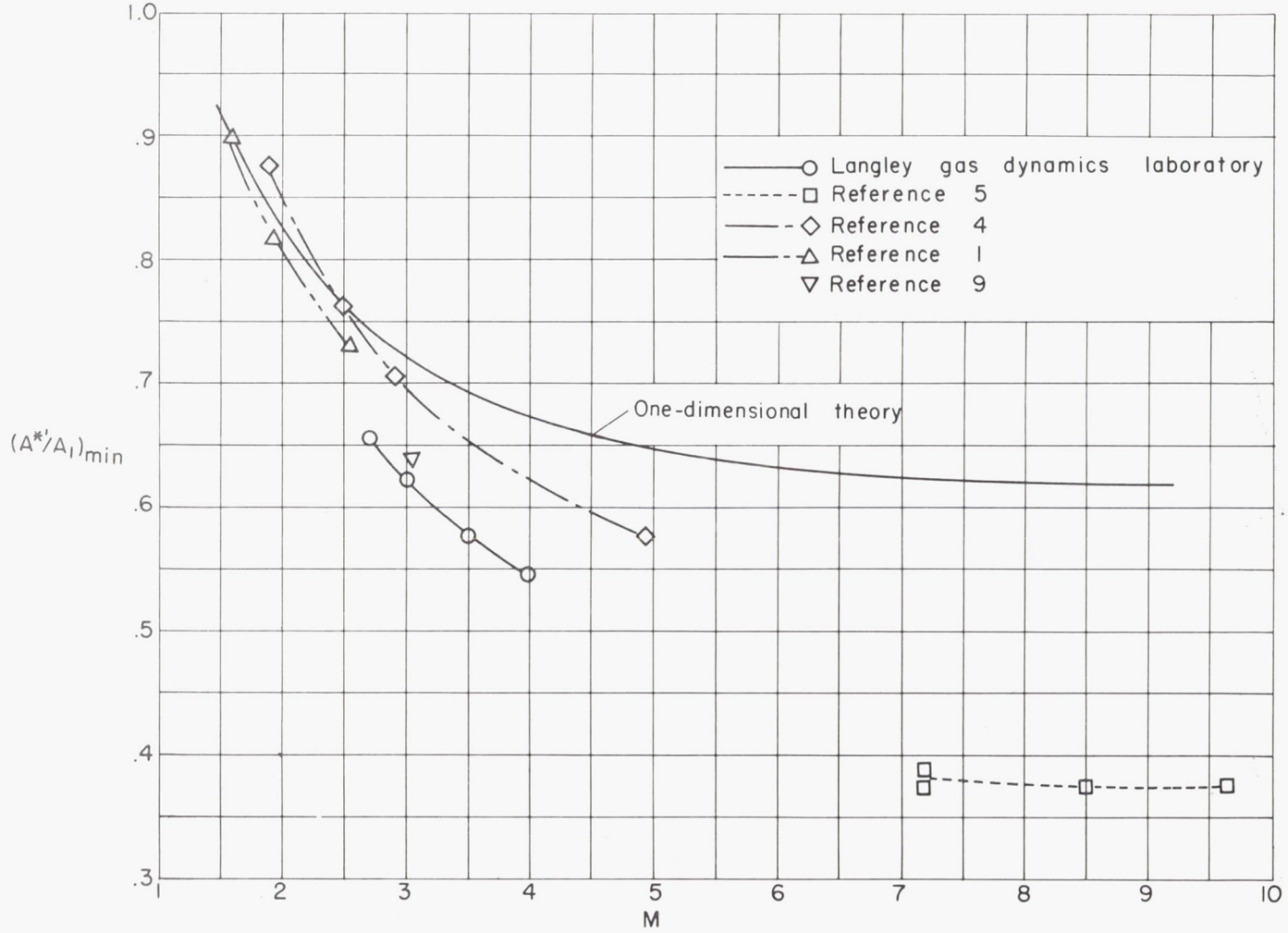

Figure 8.- Minimum value of ratio of diffuser minimum area to test-section area for which supersonic flow could be established at various Mach numbers.

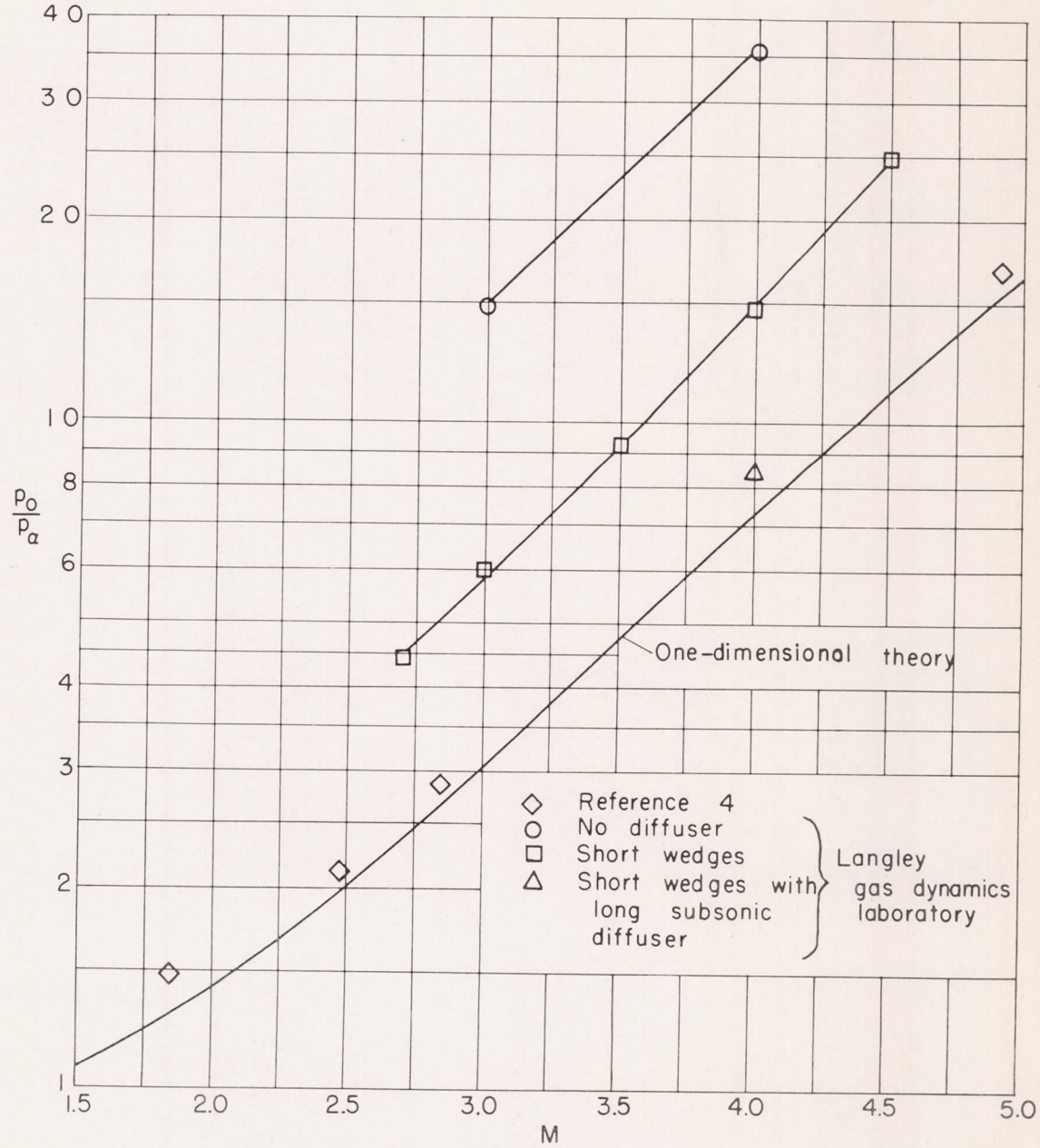

Figure 9.- Minimum values of overall pressure ratio required for starting various Mach number nozzles.

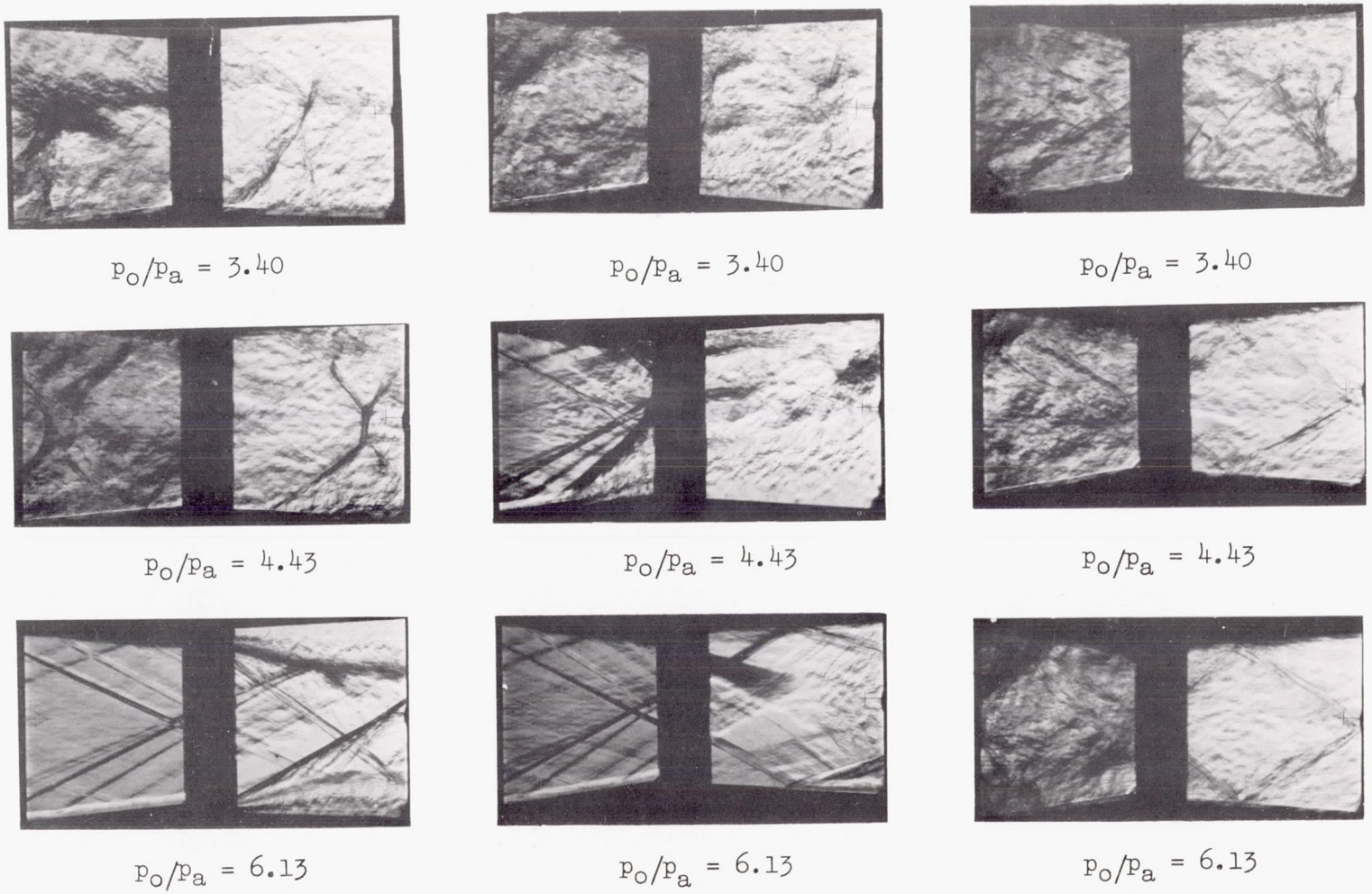

Figure 10.- Flow through wedge diffuser of M = 2.7 tunnel while starting. l/h = 1; m/h = 2.

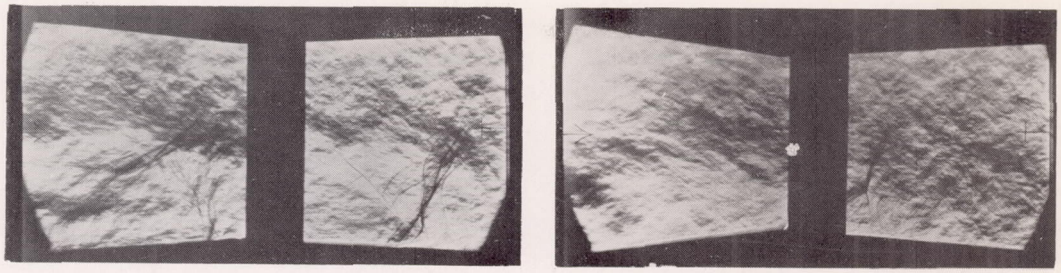

p_o/p_a = 4.43 p_o/p_a = 3.06

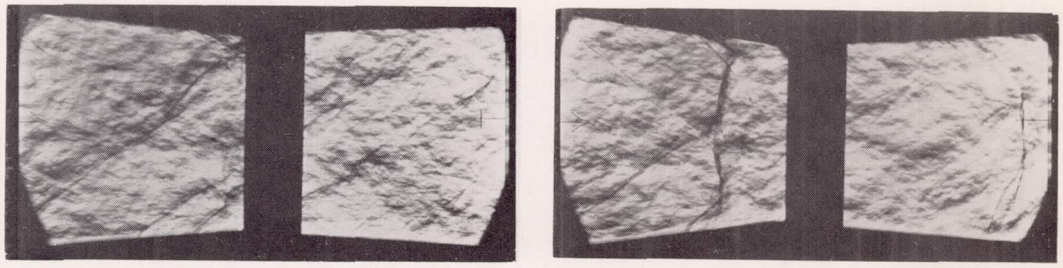

p_o/p_a = 5.78 p_o/p_a = 4.43

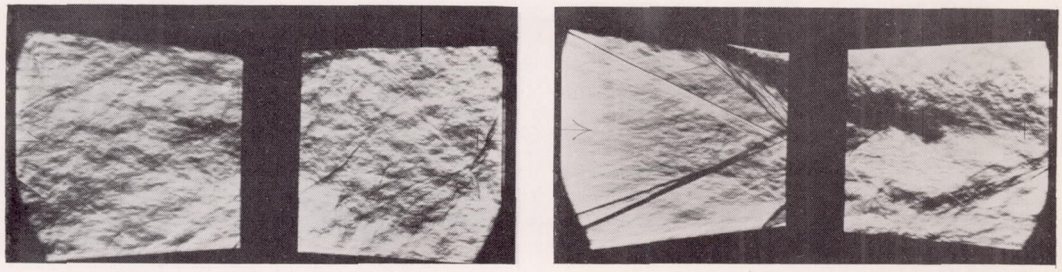

p_o/p_a = 6.47 p_o/p_a = 6.47

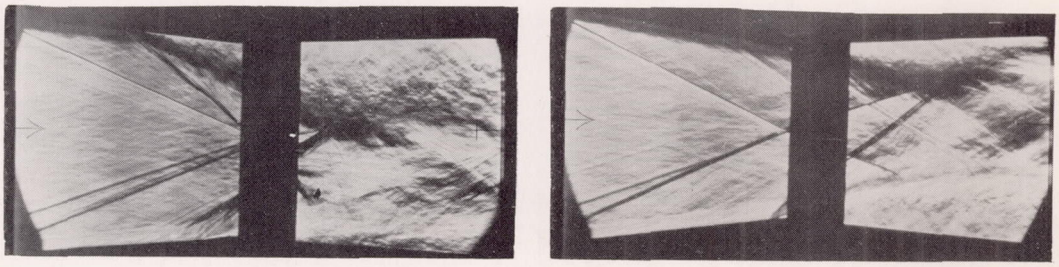

p_o/p_a = 7.84 p_o/p_a = 7.84

(a) $A^{*'}/A_1$ = 0.813. (b) $A^{*'}/A_1$ = 0.719.

L-89328.1

Figure 11.- Flow through wedge diffuser of M = 3.0 tunnel while starting. l/h = 1; m/h = 2.

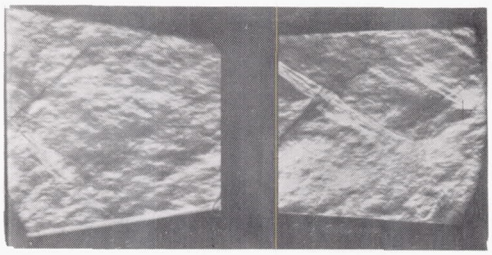

$p_o/p_a = 4.77$

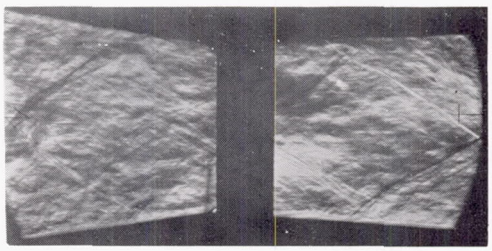

$p_o/p_a = 6.47$

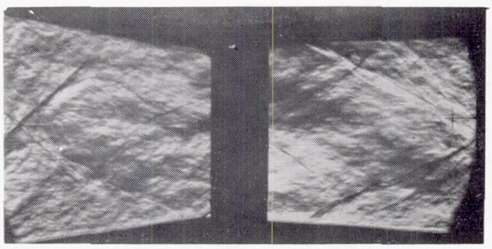

$p_o/p_a = 7.84$

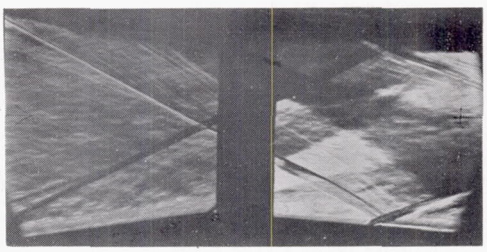

$p_o/p_a = 11.25$

L-89329.1

(c) $A^{*'}/A_1 = 0.695$.

Figure 11.- Concluded.

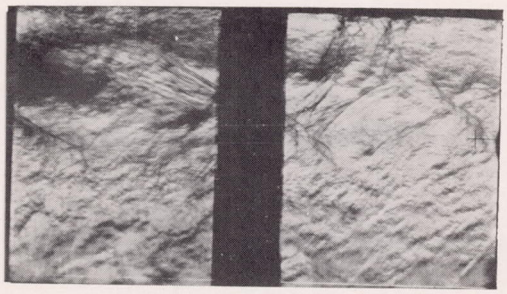

p_o/p_a = 9.54

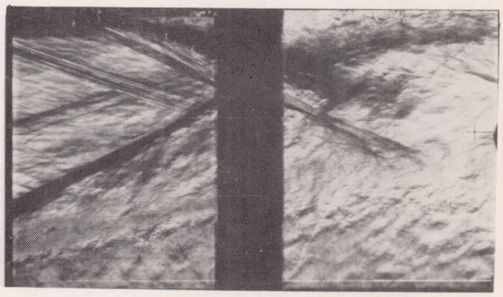

p_o/p_a = 14.65

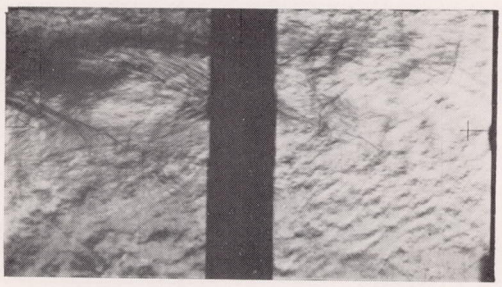

p_o/p_a = 11.25

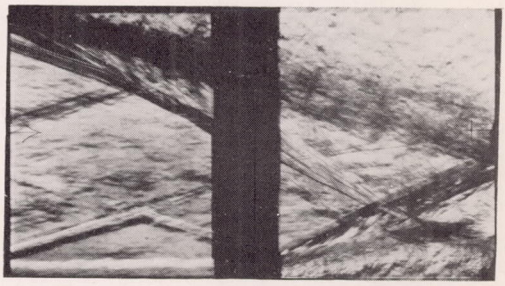

p_o/p_a = 16.35

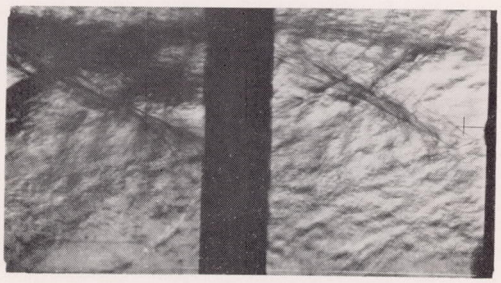

p_o/p_a = 12.95

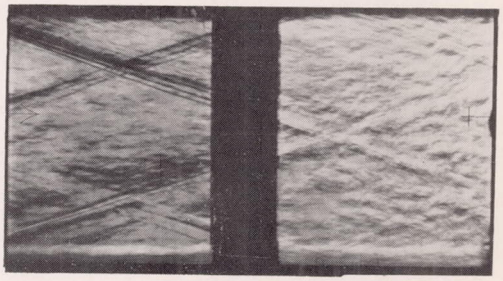

p_o/p_a = 18.05

L-89330.1

Figure 12.- Flow through straight diffuser of M = 3.5 tunnel while starting. $A^{*'}/A_1$ = 1.00.

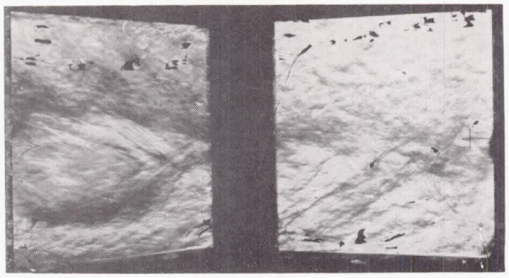

p_o/p_a = 7.84

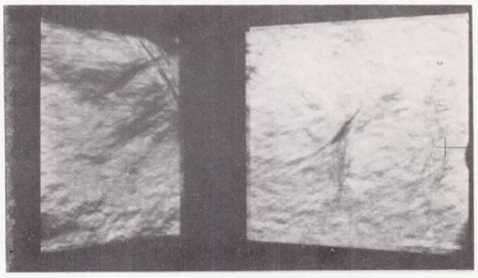

p_o/p_a = 6.13

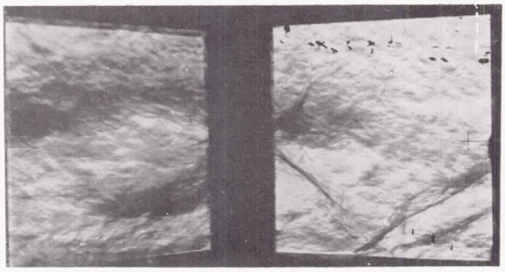

p_o/p_a = 9.54

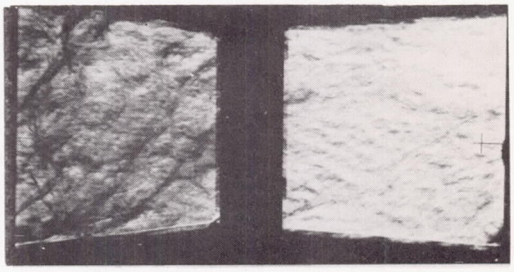

p_o/p_a = 7.84

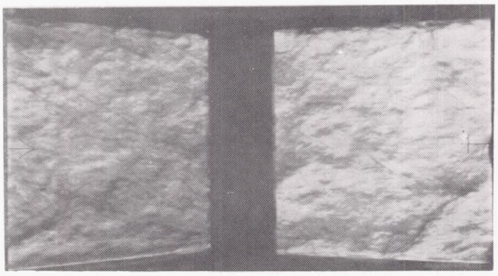

p_o/p_a = 11.25

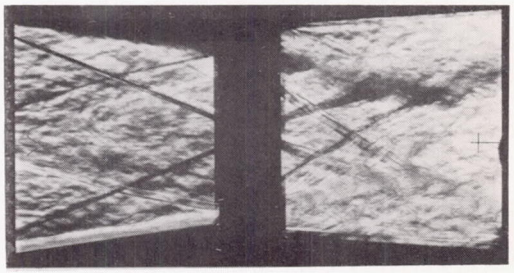

p_o/p_a = 9.54

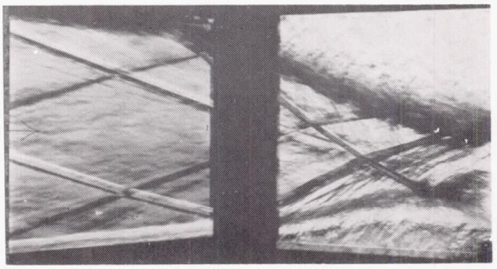

p_o/p_a = 12.95

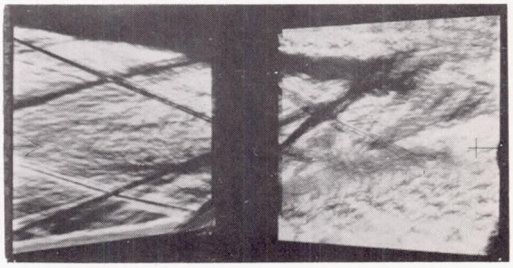

p_o/p_a = 11.25

L-89331.1

(a) $A^{*'}/A_1$ = 0.813.

(b) $A^{*'}/A_1$ = 0.719.

Figure 13.- Flow through wedge diffuser of M = 3.5 tunnel while starting. l/h = 1; m/h = 2.

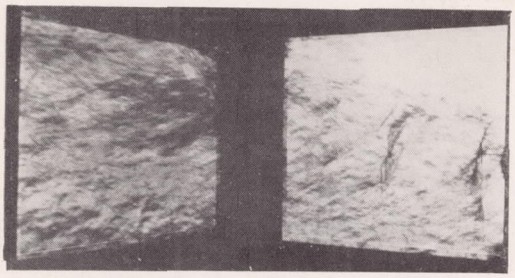

p_o/p_a = 6.13

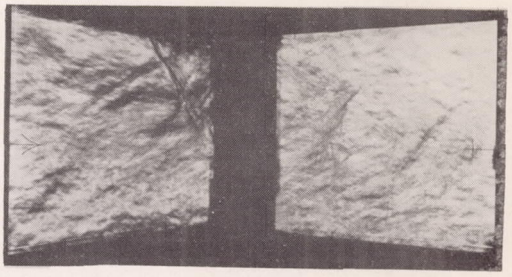

p_o/p_a = 6.13

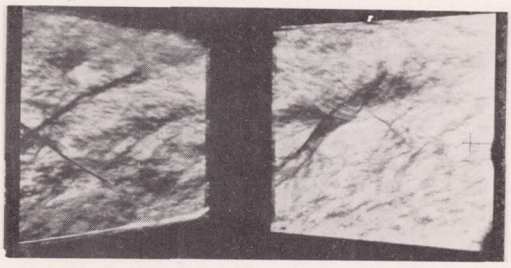

p_o/p_a = 7.84

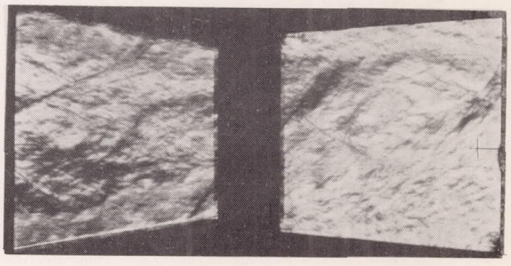

p_o/p_a = 7.84

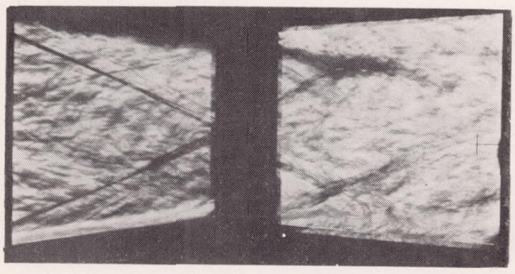

p_o/p_a = 9.54

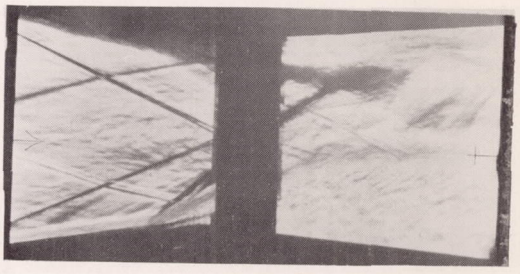

p_o/p_a = 9.54

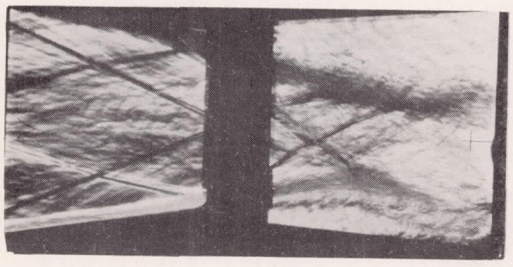

p_o/p_a = 11.25

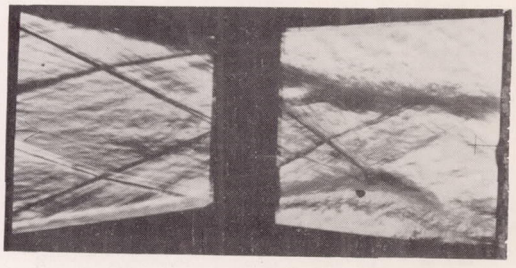

p_o/p_a = 11.25

(c) $A^{*'}/A_1$ = 0.688.

(d) $A^{*'}/A_1$ = 0.656. L-89332.1

Figure 13.- Concluded.

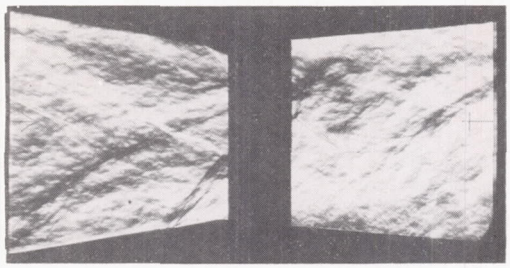

p_o/p_a = 11.25

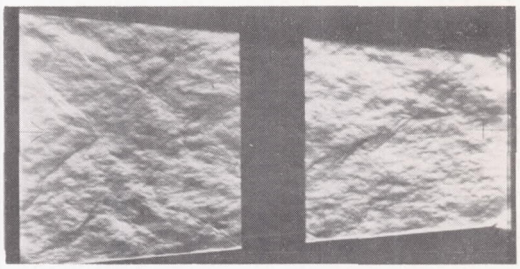

p_o/p_a = 11.25

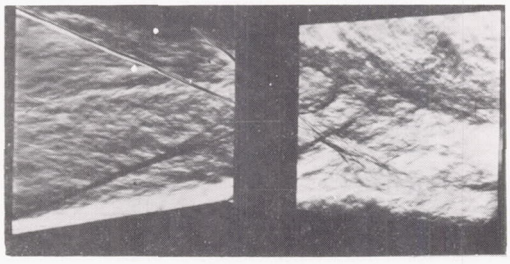

p_o/p_a = 14.65

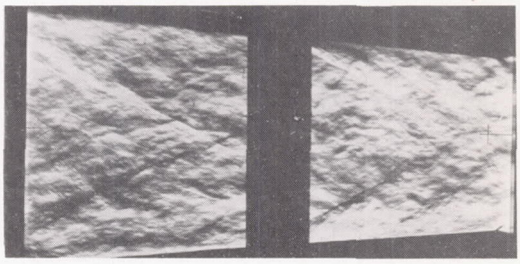

p_o/p_a = 14.65

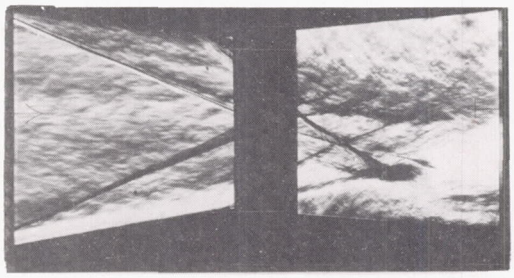

p_o/p_a = 18.05

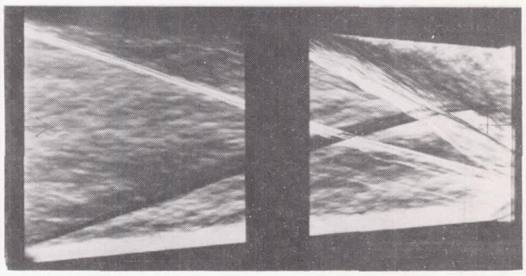

p_o/p_a = 18.05

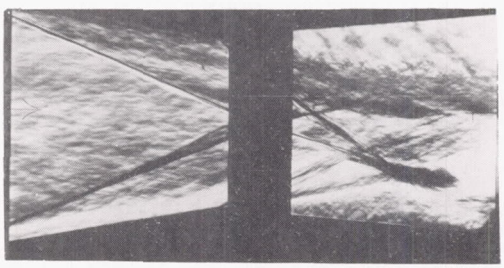

p_o/p_a = 21.45

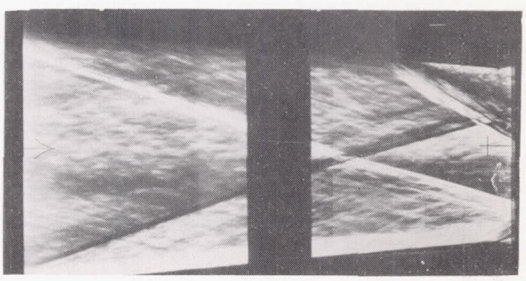

p_o/p_a = 21.45

L-89333.1

(a) $l/h = 1$; $m/h = 2$.

(b) $l/h = 2$; $m/h = 1$.

Figure 14.- Flow through wedge diffuser of M = 4.0 tunnel while starting. $A^{*'}/A_1 = 0.656$.

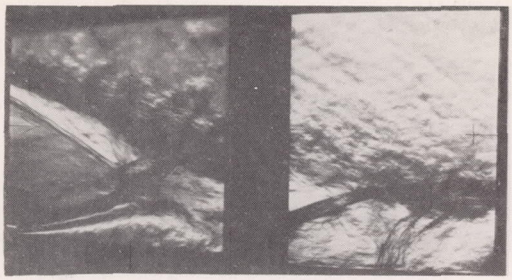

p_o/p_a = 11.25

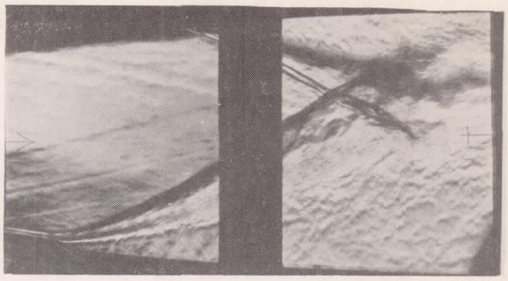

p_o/p_a = 11.25

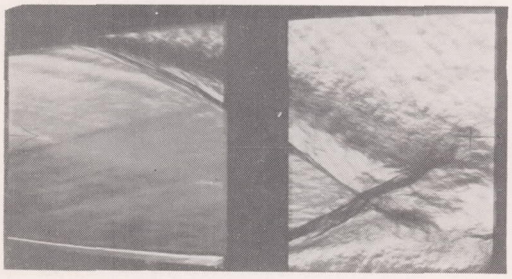

p_o/p_a = 14.65

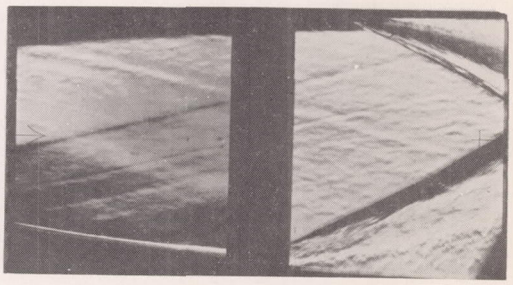

p_o/p_a = 14.65

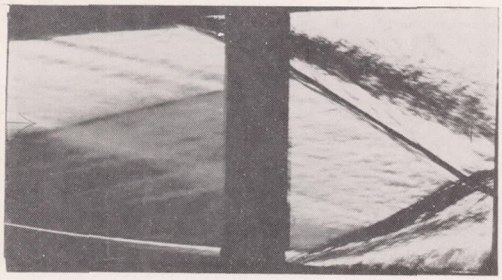

p_o/p_a = 18.05

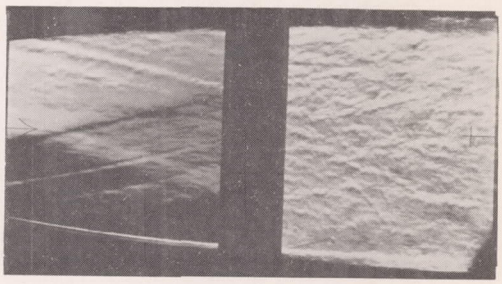

p_o/p_a = 18.05

p_o/p_a = 21.45

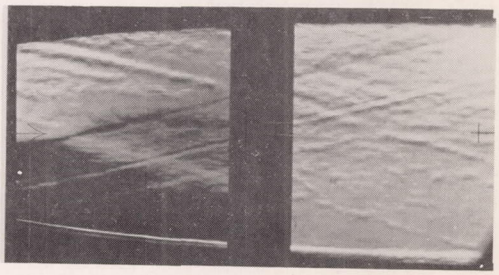

p_o/p_a = 21.45

L-89334.1

(a) $A^{*'}/A_1$ = 1.00. (b) $A^{*'}/A_1$ = 0.719; l/h = 2; m/h = 1.

Figure 15.- Flow through nozzle of M = 4.0 tunnel with wedge diffusers as extensions of nozzle contours.

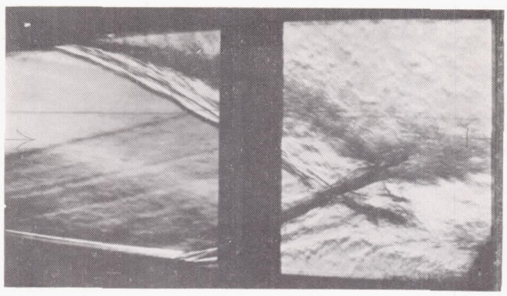

p_o/p_a = 11.25

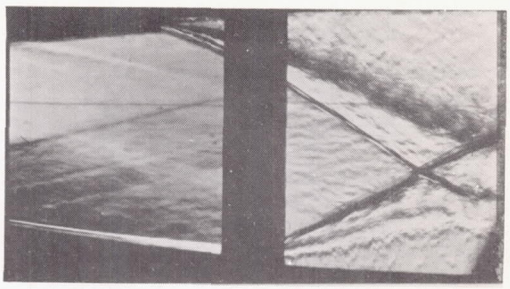

p_o/p_a = 11.25

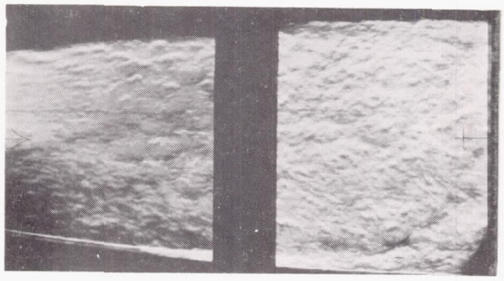

p_o/p_a = 14.65

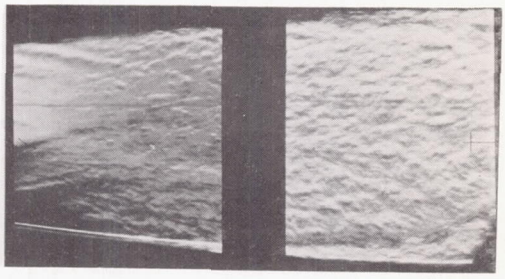

p_o/p_a = 14.65

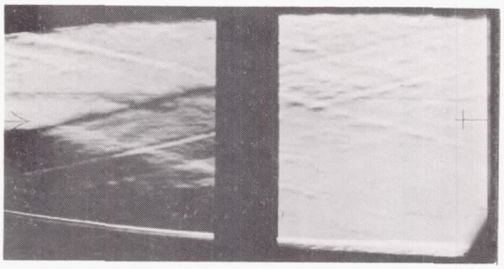

p_o/p_a = 18.05

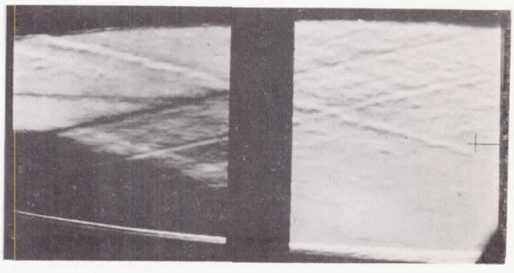

p_o/p_a = 18.05

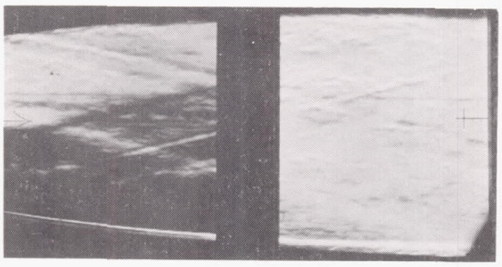

p_o/p_a = 21.45

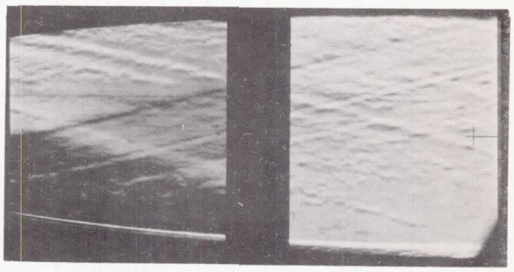

p_o/p_a = 21.45

L-89335.1

(c) $A^{*'}/A_1$ = 0.688; l/h = 2; m/h = 1.

(d) $A^{*'}/A_1$ = 0.625; l/h = 2; m/h = 1.

Figure 15.- Continued.

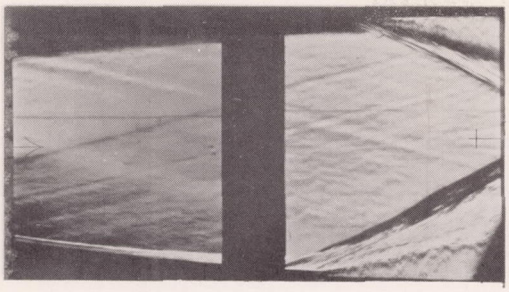

p_o/p_a = 11.25

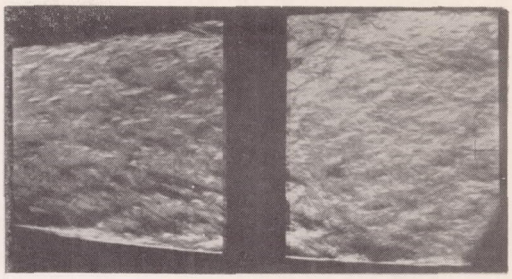

p_o/p_a = 11.25

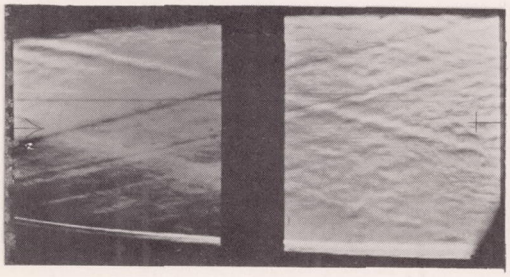

p_o/p_a = 14.65

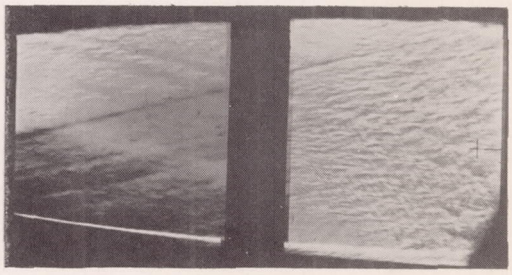

p_o/p_a = 14.65

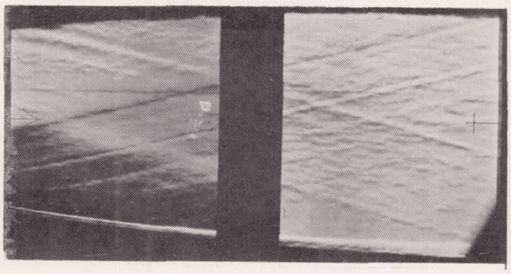

p_o/p_a = 18.05

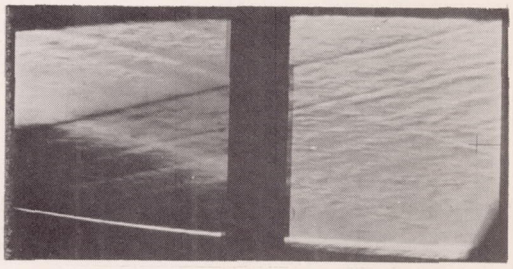

p_o/p_a = 18.05

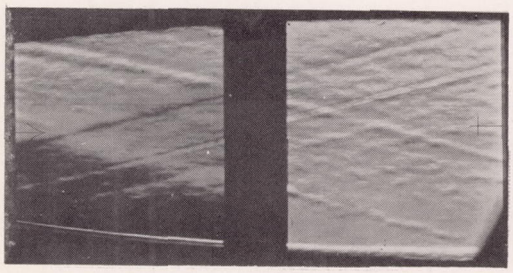

p_o/p_a = 21.45

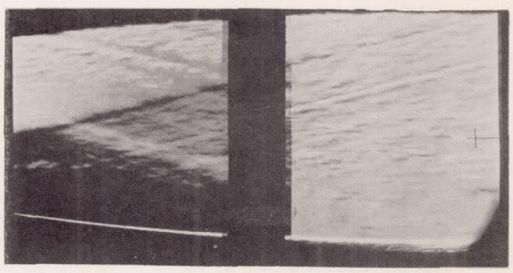

p_o/p_a = 21.45

L-89336.1

(e) $A^{*'}/A_1$ = 0.594; l/h = 2; m/h = 1.

(f) $A^{*'}/A_1$ = 0.579; l/h = 2; m/h = 1.

Figure 15.- Concluded.

Figure 16.- Variation of mass-flow parameter with Mach number.

NACA - Langley Field, Va.